

# A Novel Double-Notch Passive Hydraulic Mount Design

Reza Tikani (1), Saeed Ziaei-Rad (1), Nader Vahdati (2), Somayeh Heidari (2), Mohsen Esfahanian (1)

(1) Department of Mechanical Engineering, Isfahan University of Technology, Isfahan 84156-83111, Iran

(2) School of Mechanical and Aerospace Engineering, Nanyang Technological University, 50 Nanyang Avenue, Singapore 639798, Singapore

**PACS:** 43.40.TM Vibration isolators, attenuators, and dampers

## ABSTRACT

Passive hydraulic engine mounts are broadly applied in the automotive and aerospace applications to isolate the cabin from the engine noise and vibration. The engine mounts are stationed in between the engine and the fuselage in aerospace applications. In fixed wing turbofan engine applications, the notch frequency of each hydraulic engine mount is adjusted to either N1 frequency (engine low speed shaft imbalance excitation frequency) or to N2 frequency (engine high speed shaft imbalance excitation frequency) at the cruise condition. Since most of today's passive hydraulic engine mount designs have only one notch, isolation is only possible at either N1 or at N2, but not at both. In this paper, a novel double-notch passive hydraulic engine mount design is proposed. The new design consists of two inertia tracks. One inertia track contains a tuned vibration absorber (TVA) where the other one does not. This design exhibits two notch frequencies, and therefore can provide vibration and noise isolation at two different frequencies. The notch frequencies of the new design are easily tunable and the notches can be placed at N1 and N2 with ease. The new passive hydraulic engine mount design concept and its mathematical model are presented in details and some discussions on the simulation results are also included.

## INTRODUCTION

Passive hydraulic engine mounts are widely used in the automotive and aerospace applications for the control of cabin noise and vibration (Singh, Kim and Ravindra, 1992; Kim and Singh, 1993; 1995; Adigunaa et al., 2003; Vahdati, 2005; Christopherson and Jazar, 2006). The hydraulic mount is placed in between the engine and the fuselage, or the car engine and the car frame to reduce and control the noise and vibration level of the cabin.

Aircraft engine mounts have two main functions: 1) to connect the engine and the airframe together, and 2) to isolate the airframe from the engine vibration (Swanson, Wu and Ashrafiun,1993). Vibratory forces are mainly caused by the rotational unbalances of the engine, and result in increased stress levels in the nacelle, as well as high noise levels in the cabin (Swanson, Wu and Ashrafiun,1993). Through careful design and selection of hydraulic engine mount parameters, it is possible to select the dynamic stiffness smaller than the static stiffness at a certain frequency. This effect is called "notching" and is referred to as the minimum dynamic stiffness over a small frequency range (Yunhe, Nagi G. and Rao V., 2001).

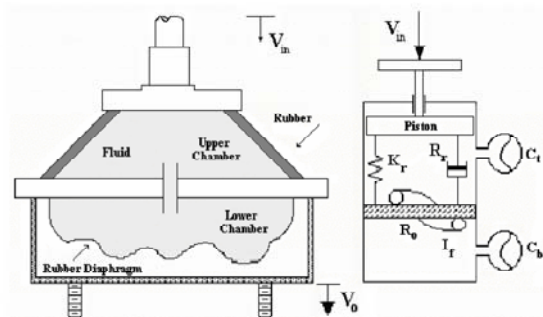
The "notch frequency" is the frequency at which the dynamic stiffness of the hydraulic mount is the lowest; therefore, greatest cabin noise and vibration reduction are obtained. The design location of the notch frequency depends on the application, but with most applications, the "notch frequency" is designed to coincide with the longest period of constant speed. For example, in the case of fixed wing applications, the notch frequency may be designed to coincide with the aircraft cruise speed rather than the take-off and the landing speeds. Since most of the airplane's flight time is spent at the cruise speed, it makes most sense to reduce the cabin noise

and vibration at the cruise speed rather than at the take-off or landing speeds (Vahdati, 2005).

The problem with existing hydraulic engine mount designs is that there is only one notch frequency and cabin noise and vibration reduction is only possible at one frequency. Here in this paper, a new hydraulic engine mount design is proposed that has two notch frequencies; therefore, cabin noise and vibration reduction is possible at two distinct frequencies.

## HYDRAULIC ENGINE MOUNT

A single-pumper passive fluid mount, as shown in Fig. 1, consists of two fluid chambers that are connected together through an inertia track.



Source: (Vahdati,1998)

**Figure 1.** A typical single pumper Hydraulic mount

The "notch frequency" location depends on inertia track length, diameter, fluid density and viscosity, and rubber stiffness. Fig. 2 shows a typical dynamic stiffness of a passive fluid mount versus frequency.

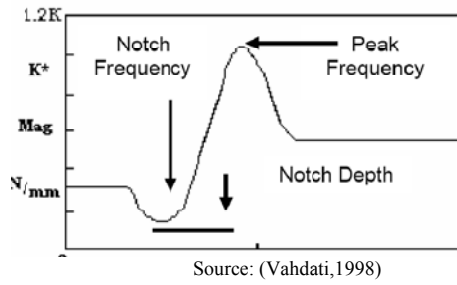


Figure 2. Dynamic stiffness of a typical hydraulic mount

But, at the cruise speed, there are many engine imbalance (disturbance) excitation frequencies and ideally one wants to isolate the cabin from all engine imbalance excitation frequencies. However, with the current hydraulic mount technology, the hydraulic mount notch frequency can only be tuned to one and only one frequency. For example, in most turbofan engines the largest imbalance excitation amplitudes normally occur at N1 (engine low-speed shaft imbalance excitation frequency) and at N2 frequencies (engine high-speed shaft imbalance excitation frequency). Since the current hydraulic mount design technology only offers isolation at one frequency, a hydraulic mount designer has no choice but to choose isolation at N1 or at N2 (Vahdati, 2005).

Literature and patent review show that only Vahdati (Vahdati, 2005)) has worked on hydraulic engine mounts that can provide vibration and noise isolation at two distinct frequencies. In his design, instead of conventional two fluid chambers, three fluid chambers and two fluid inertia tracks were used to create a double notch fluid mount.

But here, in this paper, a new single-pumper hydraulic mount design will be described, which can offer cabin noise and vibration isolation at two frequencies without a need for an additional fluid chamber. The new design concept and its mathematical model, and simulation results will be presented in the following sections.

### DOUBLE-NOTCH PASSIVE HYDRAULIC MOUNT DESIGN

Here, in this section, a double-notch passive hydraulic engine mount design concept is described, that can filter out two imbalance disturbance inputs from the cabin. Fig. 3 shows the new double-notch hydraulic engine mount design concept. In this new design, there are two fluid chambers, two inertia tracks, and a mass and two springs inside one of the inertia tracks.

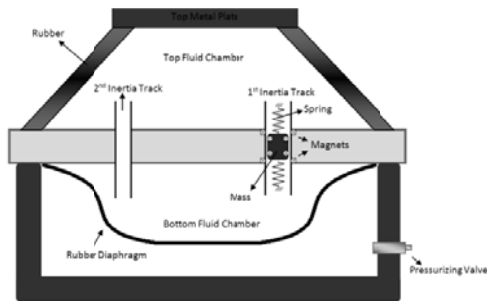


Figure 3. Double-notch passive hydraulic mount

The top fluid chamber, a customised designed rubber component (shown in Fig. 3 as a cone-shaped rubber component) acts like a spring in the axial direction, acts like a piston pumping fluid, and acts like a volumetric spring in the volumetric or bulge direction, containing the fluid. The top fluid

chamber is connected to the bottom fluid chamber via two inertia tracks. In the first inertia track, there is a mass and two springs. The fluid, flowing through the 1st inertia track, can flow in between the mass and the inertia track walls and can dynamically move the mass up and down. In the bottom fluid chamber a soft rubber diaphragm provides the volumetric stiffness and contains the fluid. This volumetric stiffness can also varied by pressuring the air behind it, as shown in Fig. 3. The bond graph model of Fig. 3 is shown in Fig. 4.

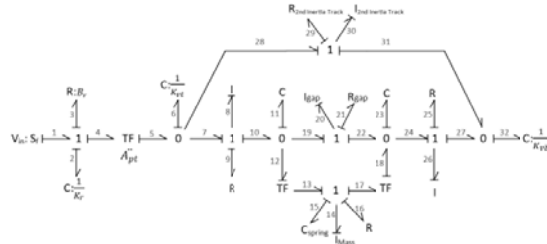


Figure 3. Bond graph model of Figure 3.

Before deriving the state space equations from the bond graph model of Fig. 3, it is necessary to obtain the flow loss and pressure drop in the inertia tracks and especially in the gap between the mass and the 1<sup>st</sup> inertia track housing.

The inertia track flow resistance, for the circular part of the 1<sup>st</sup> inertia track, is given by (Shaughnessy, Katz and Schaffer 2005)

$$R_f = \frac{128\mu L}{\pi D_{to}^4} \quad (1)$$

Where  $\mu$  is the fluid viscosity (0.0035 Ns/m<sup>2</sup>),  $D_{to}$  is the inner diameter of the inertia track and L is the length of the inertia track that is circular.

For the annular section of the inertia track, a different flow resistance equation needs to be used. The velocity profile between the cylindrical mass and the inertia track housing could be written as

$$u = \frac{r^2}{4\mu} \frac{d}{dl} (P + \gamma h) - \frac{A}{\mu} \ln r + B \quad (2)$$



Figure 4. Mass in the inertia track

Where A and B are constants and can be obtained by applying appropriate boundary conditions. In this problem, one can define boundary conditions as follows,

$$\begin{aligned} @r = a &\rightarrow u = \dot{x} \\ @r = b &\rightarrow u = 0 \end{aligned} \quad (3)$$

By considering  $\frac{d}{dl} (P + \gamma h) \cong \frac{\Delta P}{L}$ , the constants A and B will be as follows:

$$A = \frac{b^2 - a^2}{4L \ln(b/a)} \Delta P + \frac{-\mu}{\ln(b/a)} \dot{x} \quad (4)$$

$$B = \frac{(a^2 \ln b - b^2 \ln a)}{4\mu L \ln(a/b)} \Delta P + \frac{\ln a}{\ln(a/b)} \dot{x}$$

By using  $Q = \int_a^b 2\pi r u dr$ , the flow in the gap will be derived based on pressure gradient and mass velocity. The flow loss in the gap depends on the fluid flow and mass velocity and can be written as,

$$\Delta P = R_{21i} Q + R_{21ii} \dot{x} \quad (5)$$

On the other hand, the force applied to the mass by the fluid is important in the simulations. The shear stress on the mass surface is given by

$$\tau = -\mu \frac{du}{dr} \quad (6)$$

Where  $\frac{du}{dr}$  must be calculated at  $r = a$ . By Differentiating  $u$  with respect to  $r$ , the shear stress will be obtained.

$$\tau = \frac{F}{A_{\text{surf}}} = C_3 \Delta P + C_4 \dot{x} \quad (7)$$

Where  $C_3$  and  $C_4$  are

$$C_3 = \left[ \frac{b^2 - a^2}{4Lb \ln(b/a)} - \frac{b}{2L} \right] \quad (8)$$

$$C_4 = -\frac{\mu}{b \ln(b/a)}$$

The fluid force acting on the mass can be written as a function of flow and mass velocity by plugging Eq.(5) into Eq.(7).

$$F = C_3 \cdot R_{21i} \cdot A_{\text{surf}} \cdot Q + (C_3 \cdot R_{21ii} + C_4) A_{\text{surf}} \cdot \dot{x} \quad (9)$$

Now, by considering the obtained equations, the state space equations, from the bond graph model, can be derived as

$$\dot{q}_2 = V_{\text{in}} \quad (10)$$

$$\dot{q}_6 = A_{\text{pt}} V_{\text{in}} - \frac{P_8}{I_8} - \frac{P_{30}}{I_{30}} \quad (11)$$

$$\dot{P}_8 = \frac{q_6}{C_6} - R_9 \frac{P_8}{I_8} - \frac{q_{11}}{C_{11}} \quad (12)$$

$$\dot{q}_{11} = \frac{P_8}{I_8} - A_{\text{mass}} \frac{P_{14}}{I_{14}} - \frac{P_{20}}{I_{20}} \quad (13)$$

$$\dot{P}_{14} = A_{\text{mass}} \frac{q_{11}}{C_{11}} - \frac{q_{15}}{C_{15}} - A_{\text{mass}} \frac{q_{23}}{C_{23}} - R_{16i} \frac{P_{14}}{I_{14}} - R_{16ii} \frac{P_{20}}{I_{20}} \quad (14)$$

$$\dot{q}_{15} = \frac{P_{14}}{I_{14}} \quad (15)$$

$$\dot{P}_{20} = \frac{q_{11}}{C_{11}} - R_{21i} \frac{P_{20}}{I_{20}} - \frac{q_{23}}{C_{23}} - R_{21ii} \frac{P_{14}}{I_{14}} \quad (16)$$

$$\dot{q}_{23} = A_{\text{mass}} \frac{P_{14}}{I_{14}} + \frac{P_{20}}{I_{20}} - \frac{P_{26}}{I_{26}} \quad (17)$$

$$\dot{P}_{26} = \frac{q_{23}}{C_{23}} - R_{25} \frac{P_{26}}{I_{26}} - \frac{q_{32}}{C_{32}} \quad (18)$$

$$\dot{P}_{30} = \frac{q_6}{C_6} - R_{29} \frac{P_{30}}{I_{30}} - \frac{q_{32}}{C_{32}} \quad (19)$$

$$\dot{q}_{32} = \frac{P_{26}}{I_{26}} + \frac{P_{30}}{I_{30}} \quad (20)$$

The input force or effort on bond 1, is given by

$$F_{\text{in}} = \frac{q_2}{C_2} + R_3 V_{\text{in}} + A_{\text{pt}} \frac{q_6}{C_6} \quad (21)$$

In the above state space equations,  $q_2, q_6, q_{11}, q_{15}, q_{23}$  and  $q_{32}$  are the generalized displacement variables,  $P_8, P_{14}, P_{20}, P_{26}$  and  $P_{30}$  are the momentum variables. To simulate the model of Fig. 4, MATLAB Program and the above state space equations with the following baseline parameters were used.

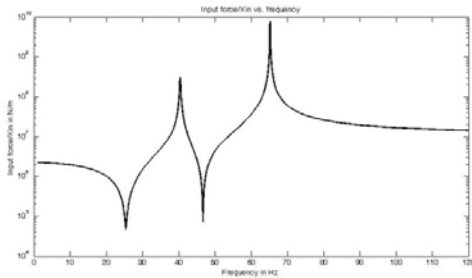
|                   |                                                                                                                           |
|-------------------|---------------------------------------------------------------------------------------------------------------------------|
| $V_{\text{in}}$   | velocity across the mount, m/s                                                                                            |
| $A_{\text{pt}}$   | effective area of the top metal, 0.009 m <sup>2</sup>                                                                     |
| $A_{\text{mass}}$ | effective area of mass in the inertia track, 2.162e-4 m <sup>2</sup>                                                      |
| $D_{\text{to}}$   | diameter of inertia track, 0.02159 m                                                                                      |
| $I_f$             | fluid inertia in the upper and below parts of inertia track, same as $I_8$ and $I_{26}$ , Ns <sup>2</sup> /m <sup>5</sup> |
| $R_f$             | inertia track flow resistance, same as $R_9$ and $R_{25}$ , Ns/m <sup>5</sup>                                             |
| $I_{fp}$          | inertia of the piston, same as $I_{14}$ , 0.0148 kg                                                                       |
| $I_{gap}$         | loss of inertia around the mass, same as $I_{20}$ ,                                                                       |
| $R_{gap}$         | flow loss in the gap, Ns/ m <sup>5</sup>                                                                                  |
| $K_r$             | axial stiffness of rubber in upper chamber ( $C_2 = 1/K_r$ ), 2.05e6 N/m                                                  |
| $B_r$             | damping component of rubber in upper chamber ( $R_3 = B_r$ ), 145 Ns/m                                                    |
| $K_{vt}$          | top chamber volumetric or bulge stiffness ( $C_6 = 1/K_{vt}$ ), 1.1e11 N/m <sup>5</sup>                                   |
| $K_{vb}$          | bottom chamber volumetric or bulge stiffness ( $C_{27} = 1/K_{vb}$ ) 2.1e9 N/m <sup>5</sup>                               |
| $K_s$             | stiffness of springs in the inertia track, ( $C_{15} = 1/K_s$ ), 2*1000 N/m                                               |
| $R_{16i}$         | flow loss around the piston ( $R_{16i} = (C_3 \cdot R_{21ii} + C_4) A_{\text{surf}}$ ), Ns/m                              |
| $R_{16ii}$        | flow loss around the piston ( $R_{16ii} = C_3 \cdot R_{21i} \cdot A_{\text{surf}}$ ), Ns/m                                |
| $I_{30}$          | fluid inertia in the 2nd inertia track, Ns <sup>2</sup> /m <sup>5</sup>                                                   |
| $R_{30}$          | 2nd inertia track flow resistance, Ns/m <sup>5</sup>                                                                      |

The fluid inertia is given by

$$I_f = \frac{\rho L}{A} \quad (22)$$

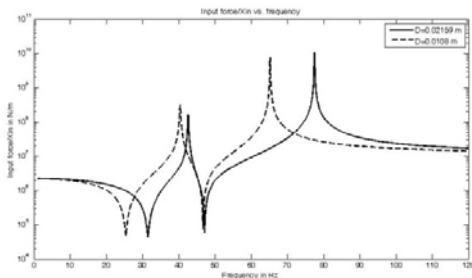
Where  $\rho$  is the fluid density (1765 kg/m<sup>3</sup>) and  $L$  is the length of upper and lower parts of the inertia track (0.0762 m). Also,  $I_{\text{gap}}$  can be calculated in the same manner (the height of the piston in the inertia track is 25.4e-3 m). The length of second inertia track is 0.2286 m and its diameter is 0.0108 m.

MATLAB program, with the above baseline parameters, was used to simulate the state space Eqs. (10) – (21). Fig. 6 shows the new hydraulic mount dynamic stiffness (defined as  $K^* = F_{in}/X_{in}$ ) versus frequency. The figure clearly shows that indeed that are two notches and two peaks. From the figure, one can see that the first and the second notch frequencies occur at 25.38 and 46.68 Hz, and the peak frequencies at 40.38 and 65.23 Hz, respectively. Of course, one can place the notch and peak frequencies to any desired location by altering the hydraulic mount parameters. The first notch location can be varied by a change in the second inertia track parameters and the second notch location by a change in the first inertia track parameters and also the mass and springs.



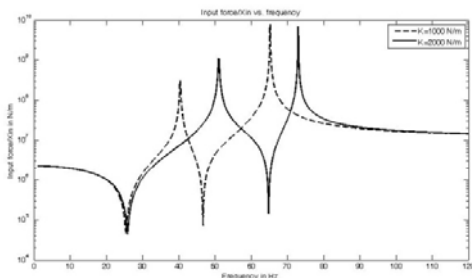
**Figure 6.** Dynamic stiffness of the double-notch hydraulic engine mount (MATLAB simulation)

For example, Fig. 7 shows that if one varies the second inertia track parameters, one can alter the location of the first notch frequency and the first and second peak frequencies. In this simulation the diameter of the second inertia track was altered from 0.0108 m to 0.02159 m.



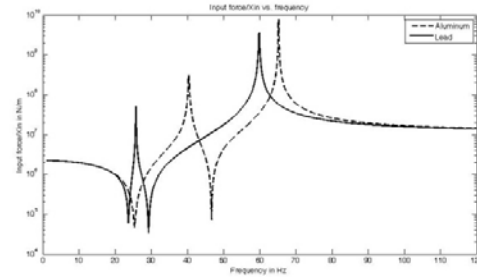
**Figure 7.** Dynamic stiffness as the diameter of the second inertia track changes

Fig. 8 shows the variation in the location of the notches and the peaks as stiffness of the springs in the inertia track is varied. In this case the second notch frequency will vary from 46.66 Hz to 64.83 Hz.



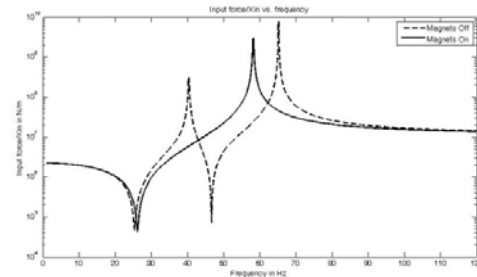
**Figure 8.** Dynamic stiffness as the stiffness of springs change

Fig. 9 shows that if one varies the piston material (lead), one can alter the location of the notch and the peak frequencies.



**Figure 9.** Dynamic stiffness as the piston material changes

In this novel design, there is an opportunity to vanish one notch by fixing the mass in the inertia track. In other words, by using magnets, one can change a double notch fluid mount design to a fluid mount design with only one notch. Fig. 10 shows the notch location in this situation.



**Figure 10.** Dynamic stiffness with and without magnets

Often, it is necessary to alter the location of the notch frequencies after the hydraulic mount is manufactured. Also, if notch frequency or frequencies need to be retuned, ideally it can be done without a need for any fluid mount redesign. Similar to the approach in (Vahdati, 2005), in this new hydraulic engine mount design, the volumetric stiffness  $K_{vb}$  can be easily varied if the gas pressure behind the rubber diaphragm is increased or decreased. This tunability can be very useful both to the original equipment manufacturer and to the customer. The two notch frequencies can be fine tuned with the help of  $K_{vb}$ ; without the need for any hydraulic mount redesign. If it is needed to fine tune the fluid mount notches in the field, one can do so by changing gas pressure. Fine tuning the notch frequencies in the field can provide better cabin noise and vibration isolation than tuning the fluid mount notches at the OEM's manufacturing site. Figs. 11 and 12 show that as the volume stiffness  $K_{vb}$  is varied, the first and second notch frequencies can be relocated.

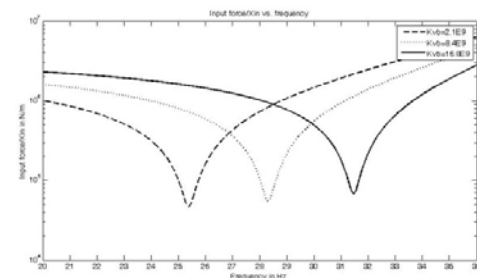


**Figure 11.** First notch frequency as the bottom volume stiffness,  $K_{vb}$ ; is varied

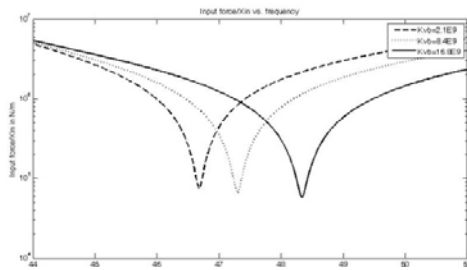


**Figure 12.** Second notch frequency as the bottom volume stiffness,  $K_{vb}$ , is varied

## CONCLUSIONS

For fixed wing applications, the current commercially available passive hydraulic engine mount designs have only one notch frequency; therefore, cabin noise and vibration isolation is only possible at N1 or at N2, but not both.

Here, in this paper, a new passive hydraulic engine mount design has been presented, which has two notch frequencies. The new design was described and its mathematical model was presented. It was shown that indeed this new design can provide vibration and noise isolation at two frequencies and one can easily tune the notch and peak frequencies by changing the gas pressure and appropriate mount parameters.

## REFERENCES

1. Adigunaa, H., M. Tiwaria, R. Singh, H. E. Tsengb and D. Hrovat (2003). "Transient Response of a Hydraulic Engine Mount." *Journal of Sound and Vibration* **268**: 217-248.
2. Christopherson, J. and G. N. Jazar (2006). "Dynamic Behavior Comparison of Passive Hydraulic Engine Mounts. Part 1: Mathematical Analysis." *Journal of Sound and Vibration* **290**: 1040-1070.
3. Kim, G. and R. Singh (1993). "Nonlinear Analysis of Automotive Hydraulic Engine Mount." *Journal of Dynamic Systems, Measurement, and Control* **115**: 482-487.
4. Kim, G. and R. Singh (1995). "A Study Of Passive And Adaptive Hydraulic Engine Mount Systems With Emphasis On Non-Linear Characteristics." *Journal of Sound and Vibration* **179**(3): 427-453.
5. Shaughnessy, E. J., I. M. Katz and J. P. Schaffer (2005). *Introduction to fluid mechanics*. New York, Oxford University Press.
6. Singh, R., G. Kim and P. V. Ravindra (1992). "Linear Analysis of Automotive Hydro-Mechanical Mount With Emphasis on Decoupler Characteristics." *Journal of Sound and Vibration* **158**(2): 219-243.
7. Swanson, D. A., H. T. Wu and H. Ashrafiuon (1993). "Optimization of Aircraft Engine Suspension Systems." *Journal of Aircraft* **30**(6): 979-984.
8. Vahdati, N. (1998). "A Detailed Mechanical Model of a Double Pumper Fluid Mount." *Journal of Vibration and Acoustics* **120** (2).

9. Vahdati, N. (2005). "Double-Notch Single-Pumper Fluid Mounts." *Journal of Sound and Vibration* **285**: 697-710.
10. Yunhe, Y. a., N. a. Nagi G. and D. Rao V. (2001). "A literature review of automotive vehicle engine mounting systems." *Mechanism and Machine Theory* **36**: 123-142.